

Increased Sensitivity to Electromagnetic and Hadronic Features of Air Showers from a New Parameterization of the Longitudinal Profiles

S. Andringa*, R. Conceição* and M. Pimenta*[†]

*Laboratório de Instrumentação e Física de Partículas, Av. Elias Garcia, 14, 1º, 1000-149 Lisboa, Portugal

[†]Departamento de Física, IST, UTL, Lisboa, Portugal

Abstract. Extensive air showers initiated by ultra-high energy cosmic rays have an almost universal longitudinal profile when the maximum energy deposition is normalized and the profile shape is translated to be centered around the depth of shower maximum. The normalization is fixed by a constant fraction of the total electromagnetic energy.

While the universality arises from a characteristic shower length, fixed by the electromagnetic cascade properties, small differences in shapes are related to the faster or slower hadronic start-up of the shower, and in particular to the nature of the primary particle. With a new parameterization for the universal shower profile, the two contributions can be separated, isolating the information regarding the hadronic interactions in a single parameter.

The distance between the depth of first interaction and the depth of shower maximum can be parameterized with the new variables, and used as a primary particle composition variable in an event-by-event analysis. Combined with the depth of shower maximum it gives access to the first interaction point and a measurement of the primary cross-sections.

Keywords: Air Shower Profile, Primary Mass Composition, Cross-Section

I. INTRODUCTION

The position of the shower maximum (X_{max}) together with the corresponding number of particles (N_{max}), proportional to the deposited energy (dE/dX_{max}), are the main characteristics of the showers as observed by Fluorescence Detectors. The full shape of the longitudinal profile can also be measured and gives information about the shower development. It is usually parameterized with two extra parameters.

The large number of electromagnetic sub-showers that constitute an extreme energy air shower initiated by protons or nuclei imply that there is some universality [1]: average behaviors that can be described statistically around the shower maximum. In this work we try to isolate the universal behaviors, the characteristic electromagnetic features of the shower, to gain access to the "hidden" hadronic features, the information about primary particle and first interactions.

We start from the usual 4-parameter Gaisser-Hillas expression [2], and expand the normalized profile around

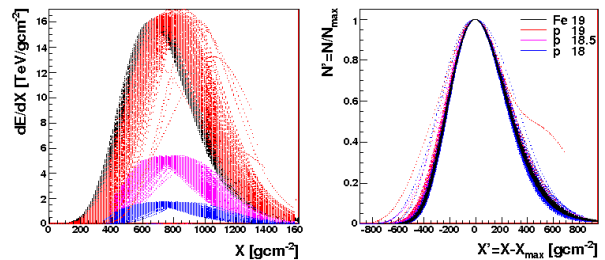


Fig. 1. Longitudinal profiles for 150 showers of different energies and primary particles, shown as $N(X)$ (left plot) and $N'(X')$ (right plot).

the shower maximum to make universality more evident. The two extra parameters are chosen to get a clear geometrical interpretation of the profile shape with experimentally accessible variables. One of the parameters is fairly constant between showers, and is related to universality, the other one is sensitive to the primary particle type. Together they give access to the full length of the shower - the distance between the shower maximum and the first interaction point. The studies were done with Conex [3] simulations of proton and iron primaries with energies from 10^{17} to 10^{20} eV. The QGSJET-II.03 [4] model was used, and then cross-checked and compared with the EPOS1.99 [5] model, in section V.

II. THE UNIVERSAL SHOWER PROFILE

The longitudinal shower profile is usually described by a Gaisser-Hillas distribution:

$$N = N_{max} \left(\frac{X - X_0}{X_{max} - X_0} \right)^{\frac{X_{max} - X_0}{\lambda}} e^{-\frac{X_{max} - X}{\lambda}} \quad (1)$$

where the number of particles, N , is described as a function of transversed depth (X in g/cm^2). N_{max} is the number of particles at the maximum, X_{max} . λ gives an indication of the interaction length, and X_0 an indication of the effective first interaction point. While N_{max} and X_{max} can be directly measured, λ and X_0 must be extracted from the profile analysis, in a strongly correlated indirect measurement.

Figure 1 shows how the profiles of several showers with different primary particles and energies become very similar when translated to the shower maximum position and normalized. We thus write the Universal

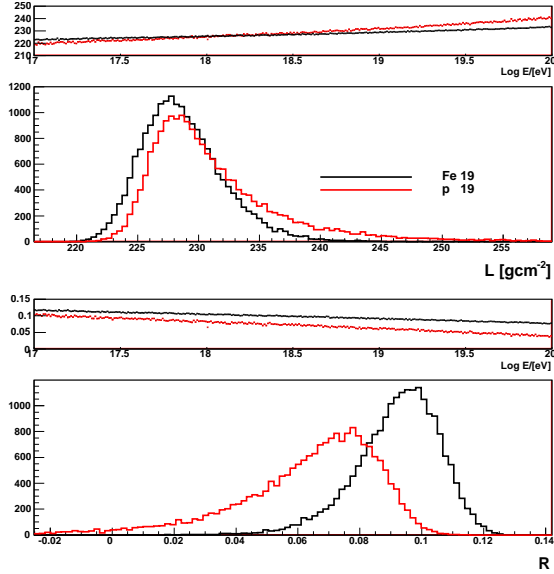


Fig. 2. Distributions of L (upper plot) and R (lower plot), in different samples at fixed energy $\log(E/eV) = 19$. The energy evolution for proton and iron primaries is also shown.

Shower Profile (USP) distribution in $N' = N/N_{max}$ and $X' = X - X_{max}$ ($X'_0 = X_0 - X_{max}$):

$$N' = \left(1 - \frac{X'}{X'_0}\right)^{-\frac{X'_0}{\lambda}} \exp\left(-\frac{X'}{\lambda}\right) \quad (2)$$

Expanding the USP around $X' \sim 0$, one gets a gaussian centered in $X' = 0$ with a width of $L = \sqrt{X'_0 \lambda}$, “rotated” (distorted) by $R = \sqrt{\lambda/X'_0}$:

$$\begin{aligned} N' &\sim \exp\left(-\frac{X'^2}{2|X'_0 \lambda|}\right) \exp\left(\frac{1}{3} \frac{X'_0}{\lambda} \left(\frac{X'}{X'_0}\right)^3\right) \\ &= \exp\left(-\frac{1}{2} \left(\frac{X'}{L}\right)^2\right) \exp\left(\frac{R}{3} \left(\frac{X'}{L}\right)^3\right) \end{aligned} \quad (3)$$

L is the main characteristic of the USP, a characteristic shower length, while R gives a first correction for the tails away from X_{max} .

The energy deposited along the shower, dE/dX , is proportional to the number of particles, N , and the integral of the distribution is used to compute the electromagnetic shower energy. The full integral of the USP is written in terms of the usual Γ function:

$$\begin{aligned} E/\frac{dE}{dX_{max}} &= \lambda A^A \exp(A) \Gamma(A+1) \\ E/\frac{dE}{dX_{max}} &\sim \lambda \sqrt{2\pi A} = \sqrt{2\pi} L, \end{aligned} \quad (4)$$

with the approximation being valid down to small values of $A = |X'_0|/\lambda = R^{-2}$, below which the total length does not comprise enough radiation lengths for the shower to have a gaussian development.

III. ELECTROMAGNETIC AND HADRONIC COMPONENTS

The universality in the shower profile comes from the electromagnetic cascade development, and the parameter

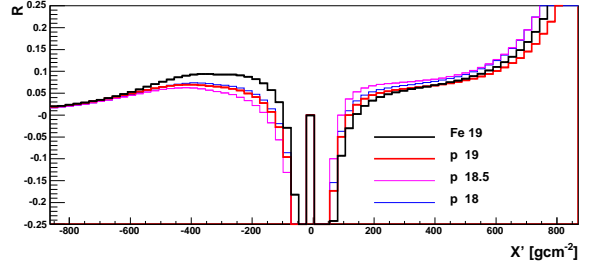


Fig. 3. Average $R(X')$ profiles for iron and proton initiated showers, calculated from eq.3 with fixed $L = 228 + 4(\log(E/eV) - 19)$ g/cm^2 .

L defined above will keep this information. This characteristic length of the shower is fixed by electromagnetic interactions, and it can not vary much either with the primary particle type or its energy. Figure 2 shows how the value of L , derived from the ratio of the electromagnetic energy to the maximum energy deposition (eq. 4), is constant within a few percent for all the samples considered. The small energy dependency can still be corrected, but dE/dX_{max} by itself is a good energy estimator.

After fixing L according to the total energy, the accuracy of the profile description in equation 3 can be checked. Figure 3 shows the average value of $R(X')$ along the shower profiles calculated by inverting eq. 3. The calculation diverges close to the gaussian peak, and a single value of R is not enough to describe the full profile shape. However, around $X' \sim 1.3 L$ ($X' \sim -300$ g/cm^2), there is a plateau where a single value of R can be chosen to characterize each shower. That defines the R which is shown in figure 2, it allows for the distinction of proton from iron primaries.

In fact, the “rotation” of the profile depends on the rate at which the energy is transferred from the hadronic to the electromagnetic component of the shower. In general, for the same energy a heavier nucleus will interact sooner and more efficiently than a proton, proton showers will start later and degrade the hadronic component in consecutive steps. The distance between the first interaction and the shower maximum must be reflected in the R parameter defined above.

IV. PRIMARY MASS AND CROSS-SECTION

There is a linear relation between the depth of shower maximum (X_{max}) and the depth of the first interaction (X_1) for constant values of R ; the full length of the shower $\Delta_0 = X_{max} - X_1$ decreases linearly as R increases, as shown in figure 4. A direct measurement of R leads to a measurement of Δ_0 , which can be combined with X_{max} to get $X_1 = X_{max} - \Delta_0$ in an event-by-event basis. Δ_0/L was checked to be an almost constant function of R , for all the studied samples: the L parameter absorbs the energy dependence.

Combining two observables, R and X_{max} , for each shower, uncorrelated measurements of cross-section and composition can be done in a model independent way. In

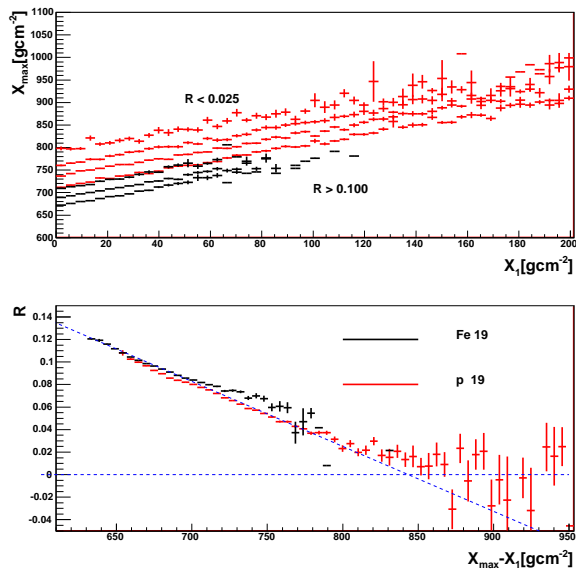


Fig. 4. X_{max} as a function of X_1 (upper plot), for different bins of R (<0.025 ; $0.025-0.050$; $0.050-0.075$; $0.075-0.100$ and >0.100) and R as a function of $X_{max} - X_1$ (lower plot), for the simulated showers initiated by proton and iron primaries of $\log(E/eV) = 19$, generated with QGSJET-II.

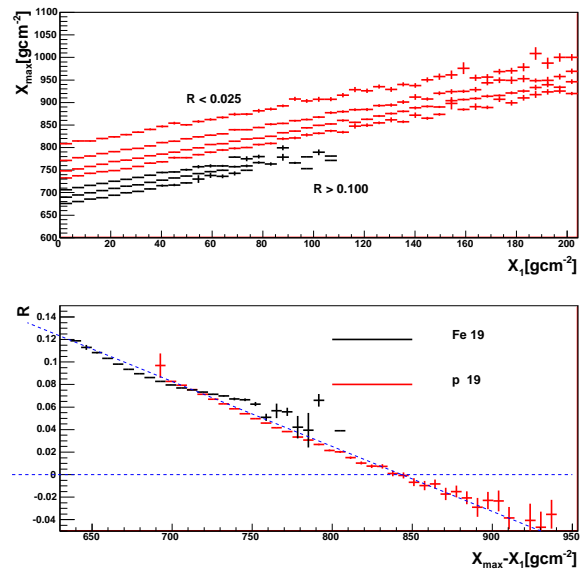


Fig. 6. X_{max} as a function of X_1 (upper plot), for different bins of R and R as a function of $X_{max} - X_1$ (lower plot), for the simulated showers initiated by proton and iron primaries of $\log(E/eV) = 19$ generated with EPOS1.9. The dotted line in the lower plot is the same as in fig.4, obtained for the QGSJET-II generator.

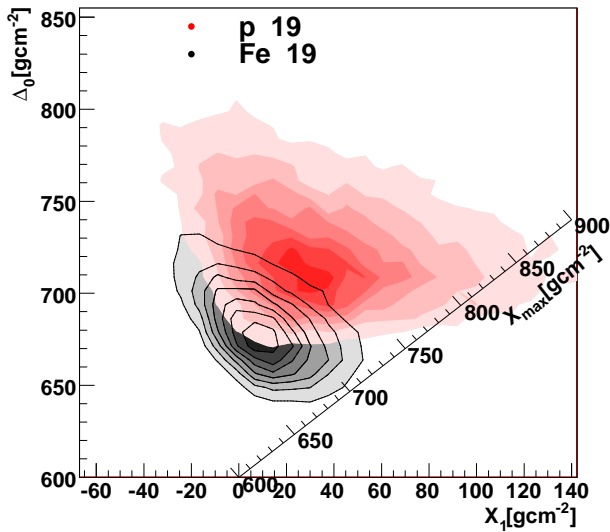


Fig. 5. X_1 and Δ_0 reconstructed from R and X_{max} for proton and iron showers at $\log(E/eV)=19$, generated with QGSJET-II. The line separated countours correspond to iron.

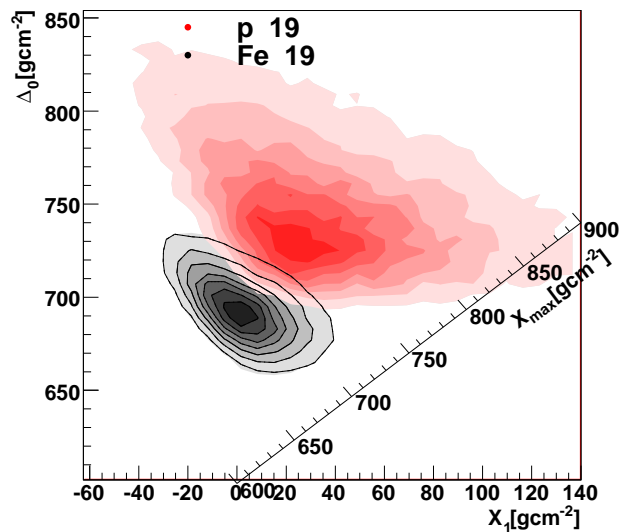


Fig. 7. X_1 and Δ_0 reconstructed from R and X_{max} for proton and iron showers at $\log(E/eV)=19$, generated with EPOS1.9. The line separated countours correspond to iron. The figure should be compared to fig.5 for the QGSJET-II generator.

fact, while X_1 depends directly on the cross-section of the first interaction, Δ_0 depends basically on the mass number of the primary particle (and on lower energy cross-sections). The discrimination between primaries can be done using both variables as shown in figure 5.

It is known that X_{max} can be used to analyze primary cosmic ray composition [6]. In fact, it has a large sensitivity for separation between primaries, as it adds the discrimination from X_1 and Δ_0 (as also shown in fig. 5), but extra information can be obtained by separating the

two contributions. X_{max} distributions have also been used to analyze primary cosmic ray cross-section [7] but, by separating the showers according to the value of R , proton (low R) and iron (high R) cross-sections can be measured separately. Even if proton and iron primaries can not be fully separated, the composition information can be recovered by the cross-section analysis.

V. TESTING DIFFERENT HADRONIC MODELS

Different hadronic models can predict different cross-sections but also different shower shapes, determined by several properties of the first interactions such as the multiplicity or the inelasticity. Information about the hadronic interactions should be reflected in the parameters L , R , Δ_0 and X_1 , but some basic characteristics should be common to all models in order to allow a model independent analysis of the data.

The above studies were done with extended air showers generated according to the QGSJET-II.03 model. In the following, they are tested using the EPOS1.99 generator. The two models differ at the level of p-A cross-sections ($\sim 10\%$ higher in EPOS), multiplicity (up to 10 times smaller in EPOS) and amount of missing energy carried by muons and neutrinos from charged pion decay ($\sim 25\%$ more muons in EPOS).

Even if this EPOS predicts a larger difference between proton and iron initiated showers, a Universal Shower Profile is again observed when translating the profiles to the shower maximum position and normalizing the maximum. L is calculated the from eq. 4. Although the distributions are slightly shifted towards higher values, and there is a noticeably higher tail for proton showers, the resulting values are compatible with the ones derived for QGSJET-II. R is then calculated from eq. 3 after fixing L as before. The peaks of the R distributions are shifted in relation to QGSJET-II ones, and the distribution for protons is significantly wider.

The relation between Δ_0 and R is a fundamental ingredient for X_1 to be derived from data. Figure 6 shows that there is still a linear relation for $\Delta_0(R)$, and that it is the same as for the QGSJET-II model. This gives better confidence that the definition of the four observables is model independent and that they can be safely extracted from data.

In figure 7, the separation between proton and iron showers in terms of X_1 , Δ_0 and X_{max} is shown for the EPOS generated showers. It should be compared with figure 5, for the QGSJET-II ones. It becomes clear that the differences between proton and iron showers are largely due to the Δ_0 values. If proton and iron showers can be separated by the analysis of X_{max} (or X_1), there is a possibility to distinguish also between different hadronic interaction models by analyzing the shower shapes and Δ_0 .

VI. CONCLUSION

Longitudinal profiles of extensive air showers can be parameterized by the shower maximum and its position, and are fairly universal after normalization and translation around the maximum. The universal shower profile can be described by a gaussian with an almost constant width slightly distorted, due to the superposition of a large number of electromagnetic sub-showers starting simultaneously or consecutively.

The normalization between the total energy and the maximum energy deposition along the shower is a constant, and fixes the characteristic electromagnetic width, $L(E)$, equal for different primary nuclei. The shape parameter, R , is different for different nuclei, and represents a new primary cosmic ray composition variable. The distance from the shower maximum to the first interaction point in the atmosphere, Δ_0 is linearly dependent on this parameter. The relation $\Delta_0(R)$ is the same for different hadronic interaction models, and can thus be applied in a model independent data analysis.

The shape parameter is a new observable, independent of the depth of shower maximum. In addition to the composition information, both observables can be combined to obtain a direct estimate of the point of first interaction. The combined analysis should allow for the measurement of primary cross-sections at high energy even in the presence of a mixed composition.

VII. ACKNOWLEDGMENTS

R.C. is supported by grant SFRH/BD/30706/2006 from FCT, Fundação para a Ciência e a Tecnologia.

REFERENCES

- [1] P. Lipari. "The Concepts of 'Age' and 'Universality' in Cosmic Rays Showers". astro-ph/0809.0190.
- [2] T.K. Gaissers and A.M. Hillas. "Reliability of the method of constant intensity cuts for reconstruction of the average development of vertical showers". Proc. of the 15th ICRC, 1977.
- [3] T. Pierog *et al.*. "First results of fast one-dimensional hybrid simulation of EAS using CONEX". Nucl.Phys.Proc.Suppl.151, 159-162, 2006. (astro-ph/0411260)
- [4] S.S. Ostapchenko. "QGSJET-II: Towards reliable description of very high energy hadronic interactions". Nucl. Phys. B (Proc. Suppl.) 151,143-146, 2006 N.N. Kalmykov, S.S. Ostapchenko and A.I. Pavlov. and "Quark-gluon string model and EAS simulation problems at ultra-high energies". Nucl. Phys. B (Proc. Suppl.) 52,17-28, 1997.
- [5] T. Pierog and K. Werner. "EPOS Model and Ultra High Energy Cosmic Rays". arXiv:0905.1198 and K. Werner, F.M. Liu and T. Pierog. "Parton ladder splitting and the rapidity dependence of transverse momentum spectra in deuteron-gold collisions at RHIC". Phys. Rev. C 74,44902, 2006.
- [6] M. Unger [Pierre Auger Coll.]. "Study of the Cosmic Ray Composition above 0.4 EeV using the Longitudinal Profiles of Showers observed at the Pierre Auger Observatory". Proc. of the 30th ICRC, 2007. (arXiv:0706.1495[astro-ph])
- [7] K. Belov [Hires Coll.]. "p-air cross-section measurement at $10^{18.5}$ -eV". Nucl.Phys.Proc.Suppl.151,197-204, 2006.